Since January 2020 Elsevier has created a COVID-19 resource centre with free information in English and Mandarin on the novel coronavirus COVID-19. The COVID-19 resource centre is hosted on Elsevier Connect, the company's public news and information website.

Original Research

Efficiency Improvements and Discovery of New Substrates for a SARS-CoV-2 Main Protease FRET Assay

SLAS Discovery
2021, Vol. 26(9) 1189–1199


DOI: 10.1177/24725552211020681
journals.sagepub.com/home/jbx
SAGE

Tonko Dražić[1*], Nikos Kühl[1*], Mila M. Leuthold[1*], Mira A. M. Behnam[1], and Christian D. Klein[1]

Abstract

The COVID-19 pandemic, caused by the SARS-CoV-2 virus, has a huge impact on the world. Although several vaccines have recently reached the market, the development of specific antiviral drugs against SARS-CoV-2 is an important additional strategy in fighting the pandemic. One of the most promising pharmacological targets is the viral main protease (M^{pro}). Here, we present an optimized biochemical assay procedure for SARS-CoV-2 M^{pro}. We have comprehensively investigated the influence of different buffer components and conditions on the assay performance and characterized Förster resonance energy transfer (FRET) substrates with a preference for 2-Abz/Tyr(3-NO_2) FRET pairs. The substrates 2-AbzSAVLQSGTyr(3-NO_2)R-OH, a truncated version of the established DABCYL/EDANS FRET substrate, and 2-AbzVVTLQSGTyr(3-NO_2)R-OH are promising candidates for screening and inhibitor characterization. In the latter substrate, the incorporation of Val at position P5 improved the catalytic efficiency. Based on the obtained results, we present here a reproducible, reliable assay protocol using highly affordable buffer components.

Keywords

biochemical protease assay, SARS-CoV-2, main protease, FRET substrate

Introduction

The coronaviruses are a group of positive-strand RNA viruses that infect mammals, birds, reptiles, and amphibians. In humans, several species of the group are important as pathogens causing various pathologies. These range from mild respiratory infections to life-threatening diseases such as severe acute respiratory syndrome (SARS). Coronaviruses are responsible for the SARS pandemic in 2002–2003, the Middle East respiratory syndrome (MERS) epidemic (ongoing since 2012), and the present COVID-19 pandemic (from 2019).[1–3] The viral disease COVID-19 is caused by SARS-CoV-2, which was first described in Wuhan, China, in December 2019.[4] The present worldwide pandemic has, as of January 25, 2021, affected more than 99 million persons, with more than 2.1 million reported deaths.[5] In around 80% of the symptomatic infections, a mild disease with fever or mild pneumonia can be observed. Fourteen percent of the cases are more severe, and about 5% of the patients have to be treated in intensive care units.[6] The infection appears to be mainly transmitted by aerosols during social interactions.[7]

Specific antiviral drugs against infections with SARS-CoV-2 and other coronaviruses have not yet been approved. The main protease, M^{pro} ($3CL^{pro}$, nsp5), of coronaviruses has no closely related homologs in humans, is involved in an essential step of the viral life cycle, and is therefore considered a promising drug target.[8] M^{pro} is a chymotrypsin-like cysteine protease that cleaves the viral polyprotein into several functional proteins. The relevant proteolytic species is the dimer of the protease.[9] M^{pro} cleaves the polyproteins exclusively after glutamine residues at 11 sites.[8,10,11] A number of compounds have been described to act as inhibitors of coronaviral M^{pro}. These frequently have a

[1]Medicinal Chemistry, Institute of Pharmacy and Molecular Biotechnology IPMB, Heidelberg University, Heidelberg, Germany

Received Feb 19, 2021, and in revised form May 4, 2021. Accepted for publication May 10, 2021.

*These authors contributed equally to this work.

Corresponding Author:
Christian D. Klein, Medicinal Chemistry, Institute of Pharmacy and Molecular Biotechnology IPMB, Heidelberg University, Im Neuenheimer Feld 364, Heidelberg, 69120, Germany.
Email: c.klein@uni-heidelberg.de

peptidic structure and contain an electrophilic group to promote covalent binding to the catalytic cysteine.[12–17]

Biochemical assays are valuable tools to study viral proteases and to identify, develop, and optimize protease inhibitors. A frequently used, high-throughput-capable technique to investigate the activity of proteases is Förster resonance energy transfer (FRET)-based assays. In FRET, the energy of an excited donor group is transferred to an acceptor moiety in close proximity, the "quencher." The energy transfer is radiation-free and does not involve intramolecular emission and absorption of photons. By incorporation of a FRET pair into an enzyme substrate, the cleavage rate of the substrate can be investigated.[18,19]

We herein present the development and optimization of a biochemical FRET-based SARS-CoV-2 M^{pro} assay. Several assay conditions and additives such as salts, polyols, and detergents were studied. Furthermore, several established and new FRET substrates were synthesized, compared, and tested, aiming to provide a robust and cost-effective protocol that can be carried out under a wide range of infrastructural conditions.

Materials and Methods

General Comments

FRET substrates were synthesized via the Fmoc (fluorenylmethyloxycarbonyl protecting group) solid-phase peptide synthesis (SPPS) protocol, as described in the supplemental information. Other chemicals were purchased from commercial suppliers. Boceprevir was obtained from Biosynth-Carbosynth (Bratislava, Slovak Republic). The measurements were performed in black 96-well V-bottom plates (Greiner Bio-One, Germany) using a BMG Labtech Fluostar OPTIMA microtiter fluorescence plate reader at an excitation wavelength of 330 nm and an emission wavelength of 430 nm. All measurements were performed at room temperature.

Construct Design

The expression construct for the SARS-CoV-2 M^{pro} was designed by multiple sequence alignment of the Wuhan seafood market pneumonia virus isolates 2019-nCoV (accession numbers MN938384.1, MN975262.1, MN988713.1, and MN985325.1). The reading frame for the SARS-CoV-2 M^{pro} was determined by alignment with previous SARS-CoV M^{pro} expression constructs.[20] Codon usage was optimized individually for optimized expression in both *Escherichia coli* and eukaryotic systems. The gene sequence coding for the SARS-CoV-2 M^{pro} protease was ordered at Eurofins with *Not*I and *Bam*HI restriction sites at the 3′ and 5′ ends, respectively. The gene sequence encoding the SARS-CoV-2 M^{pro} was inserted by restriction-based cloning into a pET28a(+) expression vector to obtain a C-terminal His-tag. The C-terminal His-tag was chosen because a structural analysis of SARS-CoV M^{pro} indicated less disruption of dimerization in the presence of a C-terminal tag compared with an N-terminal tag. The cleavage inactive mutant C145A was cloned from the wild-type construct by molecular assembly with two sets of primers. The identity of the constructs was determined by agarose gel electrophoresis, colony PCR, and sequencing.

Expression and Purification of SARS-CoV-2 M^{pro}

The plasmid encoding the SARS-CoV-2 M^{pro} was transformed into *E. coli* BL21 DE3 cells for expression. Overnight culture from a single colony was grown by shaking at 37 °C in LB medium supplemented with 50 mg/mL kanamycin. On the next day, prewarmed LB medium with kanamycin was mixed 1:40 with overnight culture and bacteria were grown until the optical density (OD) at 600 nm reached 0.3–0.4. Subsequently, the temperature was reduced to 25 °C. Protein expression was induced by addition of 1 mM isopropyl-D-thiogalactoside (IPTG), and cells were further grown by shaking for 24 h at 25 °C. Bacteria were harvested by centrifugation, and the resulting cell pellet was flash frozen in liquid nitrogen and stored for further use at –80 °C.

Purification of the SARS-CoV-2 M^{pro} was performed on ice or at 4 °C. One gram of cell pellet was thawed and resuspended in 10 mL of ice-cold buffer A (20 mM Tris, 200 mM NaCl, 10 mM imidazole, pH 7.6). The bacteria were lysed using a high-pressure cell disrupter (One Shot, Constant Systems LTD). Cell debris was centrifuged 2 h at 50,000*g* to remove insoluble aggregates and inclusion bodies. The supernatant was mixed after centrifugation with 1 mL of preequilibrated (buffer A) Ni-NTA-beads and incubated on a rolling shaker for 30 min at 4 °C. Subsequently, the Ni-NTA-beads were washed with buffer A, containing increasing concentrations of imidazole (10 mM, 20 mM, 50 mM, pH 7.6; 10–20 mL buffer per step). The protein was eluted by multiple elution steps, each with 1 mL of buffer B (20 mM Tris, 200 mM NaCl, 500 mM imidazole). Elution fractions were analyzed by OD measurement and sodium dodecyl sulfate–polyacrylamide gel electrophoresis (SDS-PAGE). Fractions containing the SARS-CoV-2 M^{pro} were concentrated and buffer was exchanged with buffer C (20 mM Tris, 200 mM NaCl, 1 mM DTT, 1 mM EDTA, pH 7.6) using Amicon centrifugation filters. Protein was further purified by size-exclusion chromatography using an S200 column and buffer C as running buffer. Fractions with pure protein were concentrated and mixed with 50% sterile glycerol, and aliquots at 8 mg/mL (~228 μM) were flash frozen in liquid nitrogen and stored at –80 °C until further use.

Evaluation of Assay Buffer Composition

Buffering compounds, salts, additives, polyols, and detergents were evaluated by preparing a buffer solution with corresponding concentrations of the components. In the experiment evaluating the buffer components, 50 mM Tris-HCl, phosphate, and HEPES buffer were prepared without the addition of other components at pH 7.5. In the experiment with salts and additives, 50 mM Tris-HCl buffer, pH 7.4, was used with the addition of NaCl at various concentrations (50 mM, 100 mM, or 150 mM), 1 mM DTT, 1 mM TCEP, or 1 mM EDTA. For the evaluation of polyols, ethylene glycol (10%, 20%, or 30% v/v) or glycerol (10%, 20%, or 30% v/v) was added to the 50 mM Tris-HCl buffer, pH 7.4. The influence of detergents was evaluated using 50 mM Tris-HCl buffer, pH 7.4, with the addition of 0.01% detergent. In all experiments, the prediluted solution of M^{pro} was prepared by pipetting the corresponding volume of the enzyme storage buffer (enzyme concentration 228 μM) and adding the tested buffer to obtain an enzyme concentration of 5 μM. Substrate **4** was diluted from a stock solution (10 mM in DMSO) in distilled water to obtain a concentration of 500 μM. The prediluted solution of enzyme (5 μM, 10 μL) was pipetted into the wells, followed by the corresponding buffer (80 μL). Reactions were initiated by the addition of the substrate solution (10 μL). The final M^{pro} concentration in the assay was 500 nM, and the concentration of the substrate was 50 μM. Please note that the concentrations of the investigated assay components (salt, detergent, polyols) were slightly lower in the final assay buffer than in the buffer solutions described above. The final concentrations are indicated in **Figure 1**. The final volume was 100 μL per well. The enzymatic activity was monitored for 15 min and determined as a slope of relative fluorescence units per second (RFU/s) for each assay additive and component. The results are expressed relative to the Tris-HCl buffer (without other components), as a mean of the triplicates and the respective standard deviation. In each measurement, a corresponding solution without the addition of the protease was used as a negative control.

Evaluation of pH Value

The assay buffer (50 mM Tris-HCl, 100 mM NaCl, ethylene glycol [20% v/v], 0.0016% Brij 58) was prepared with the pH value varying by 0.2 units in the range 7.0–8.0. The prediluted solution of the protease was prepared by pipetting the required volume of the enzyme in storage buffer (enzyme concentration 228 μM) and adding the assay buffer, pH 7.4, to obtain an enzyme concentration of 10 μM. The prediluted solution of substrate **4** was prepared by adding the substrate stock solution (10 mM in DMSO) into the assay buffer, pH 7.4, to obtain a substrate concentration of 1 mM. The prediluted solution of enzyme (5 μL) was added into the wells, after which the assay buffer with the corresponding pH value was added (90 μL). The measurements were initiated by the addition of the substrate solution (5 μL). The final M^{pro} concentration in the assay was 500 nM, and the concentration of the substrate was 50 μM. The final volume was 100 μL per well. The enzymatic activity was monitored for 15 min and determined as a slope of relative fluorescence units per second for each pH value. The results are expressed relative to the assay buffer, pH 7.0, as a mean of the triplicates and the respective standard deviation. In each measurement, a corresponding solution without the addition of the protease was used as a negative control.

Evaluation of Protease Concentration

The prediluted solution of protease was prepared by pipetting the corresponding volume of the enzyme storage buffer (enzyme concentration 228 μM) and adding the assay buffer (50 mM Tris-HCl, pH 7.4, 100 mM NaCl, ethylene glycol [20% v/v], 0.0016% Brij 58) to obtain an enzyme concentration of 5 μM. The prediluted solution of substrate **4** was prepared by adding the substrate stock solution (10 mM in DMSO) to the assay buffer to obtain a concentration of 500 μM. The prediluted enzyme solution (1–8 μL) was added to the wells, after which the assay buffer was added (82–89 μL). The measurements were initiated by the addition of the substrate solution (10 μL). The final M^{pro} concentrations in the assay were 0 nM, 50 nM, 100 nM, 200 nM, 300 nM, and 400 nM, and the concentration of the substrate was 50 μM. The final volume was 100 μL per well. The enzymatic activity was monitored for 15 min and determined as a slope of relative fluorescence units per second for each enzyme concentration. The results are expressed as relative fluorescence units per second, as a mean of the triplicates and the respective standard deviation.

Evaluation of Substrates

The M^{pro} prediluted solution (prepared in assay buffer) was pipetted in the wells (10 μL), followed by assay buffer (80 μL, 50 mM Tris-HCl, pH 7.4, 100 mM NaCl, ethylene glycol [20% v/v], 0.0016% Brij 58). Reactions were initiated by the addition of 10 μL of the corresponding substrates (prepared in the assay buffer). The final protease concentration in the assay was 300 nM, whereas the concentration of the substrate was 50 μM. The final volume was 100 μL per well. The enzymatic activity was monitored for 15 min and determined as a slope of relative fluorescence units per second for each substrate. The results are expressed as relative fluorescence units per second, as a mean of the triplicates and the respective standard deviation. In each measurement, a corresponding solution without the addition of the protease was used as a negative control.

Kinetic Measurements

The required volumes of prediluted selected substrates, dissolved in assay buffer, to yield final concentrations in the

range of 0–400 µM were pipetted into the wells, followed by a corresponding volume of the assay buffer (50 mM Tris-HCl, pH 7.4, 100 mM NaCl, ethylene glycol [20% v/v], 0.0016% Brij 58). Reactions were initiated by the addition of 10 µL of the prediluted protease (prepared in assay buffer) to obtain a final enzyme concentration of 300 nM. The final volume was 100 µL per well. The enzymatic activity was monitored for 15 min and determined for each concentration as a slope of relative fluorescence units per second. The obtained values were divided by the correction factor for each concentration. Additional details are provided in the supplemental information (see **Suppl. Fig. S2, Suppl. Tables S1–S4**). For the calculations, the enzymatic activity was expressed as micromoles per second. The mean and the standard deviation of the triplicates plotted against the corresponding concentration were used to calculate the K_m and V_{max} values in Prism 6.01 (Graphpad Software, Inc.) using the Michaelis–Menten fit.

Z′ Value Determination

The M^{pro} prediluted solution (final concentration 300 nM) together with the assay buffer (50 mM Tris-HCl, pH 7.4, 100 mM NaCl, ethylene glycol [20% v/v], 0.0016% Brij 58) was pipetted in 47 wells. The same volume of the assay buffer without the protease was pipetted in 48 wells. After 15 min of preincubation, substrate **1** (final concentration 25 µM; prepared from 10 mM DMSO stock solution) was added to all wells. The final volume was 100 µL per well. The enzymatic activity was monitored for 15 min and determined as a slope of relative fluorescence units per second. Z′, signal window (SW), and assay variability ratio (AVR) values were calculated as described in literature.[21,22]

SARS-CoV-2 Main Protease Relative Inhibition Assay

The prediluted solutions of the reference compounds (500 µM) were obtained by diluting the compound stock solution (10 mM in DMSO) in the assay buffer (50 mM Tris-HCl, pH 7.4, 100 mM NaCl, ethylene glycol [20% v/v], 0.0016% Brij 58). The prediluted solution of protease (3 µM) was prepared by adding the corresponding volume of the assay buffer to the enzyme storage buffer (enzyme concentration 228 µM). The prediluted solution of the protease (10 µL), the assay buffer (60 µL), and the prediluted solution of the inhibitor (10 µL) were incubated for 15 min. The reaction was initiated by the addition of 20 µL of the prediluted solution of FRET substrate **1** (concentration 125 µM), which was prepared from the substrate stock solution (10 mM in DMSO) and the assay buffer. The final enzyme concentration in the assay was 300 nM, the compound concentration was 50 µM, and the concentration of the substrate was 25 µM. The final volume was 100 µL per well. The enzymatic activity was monitored for 15 min and determined as a slope of relative fluorescence units per second for each compound. Percentage inhibition was calculated relative to a positive control (without the inhibitor), as a mean of the triplicates and the respective standard deviation.

SARS-CoV-2 M^{pro} Assay for IC_{50} Determination. Eight inhibitor concentrations with 1:2 serial dilutions and covering the range 0–10 or 0–200 µM were studied. The prediluted inhibitor solutions were prepared by diluting the compound stock solution (10 mM in DMSO) in the assay buffer (50 mM Tris-HCl, pH 7.4, 100 mM NaCl, ethylene glycol [20% v/v], 0.0016% Brij 58). The prediluted solution of protease (3 µM) was prepared by adding the corresponding volume of the assay buffer to the enzyme storage buffer (enzyme concentration 228 µM). The prediluted solution of the M^{pro} (10 µL), the assay buffer (60 µL), and the prediluted solution of the inhibitor (10 µL) were incubated for 15 min. The reaction was initiated by the addition of 20 µL of the prediluted solution of FRET substrate **1** (concentration 125 µM), which was prepared from the substrate stock solution (10 mM in DMSO) and the assay buffer. The final M^{pro} concentration in the assay was 300 nM, and the concentration of the substrate was 25 µM. The final volume was 100 µL per well. The enzymatic activity was monitored for 15 min and determined as a slope of relative fluorescence units per second for each concentration. The mean and the standard deviation of the triplicates plotted against the corresponding concentration were used to determine the IC_{50} values in Prism 6.01 (Graphpad Software, Inc.) using nonlinear dose–response curves with variable slopes.

Results and Discussion

Assay Conditions

In order to find the optimal assay conditions, measurements with substrate **4** (see below) and various assay conditions as well as buffer components were carried out (**Fig. 1**). First, the influence of different buffers was investigated. Most SARS-CoV-2 M^{pro} biochemical assays were conducted using Tris buffer[10,13–16,23–25] or HEPES buffer.[12,26,27] We found no significant difference between Tris and phosphate buffer, whereas the fluorescence increase over time was lower when using a HEPES buffer (**Fig. 1A**). Next, the addition of different salt concentrations was examined. The ionic strength had no obvious influence on substrate cleavability. This is in contrast to a previously published study on SARS-CoV M^{pro}.[28] Other additives like the reducing agents dithiothreitol (DTT) and tris(2-carboxyethyl)phosphine (TCEP) led to higher enzyme activity (**Fig. 1B**). Reducing agents are often included in buffers for enzyme storage, purification, and biochemical assays to prevent cysteine oxidation. However, electrophilic inhibitors that are reactive toward

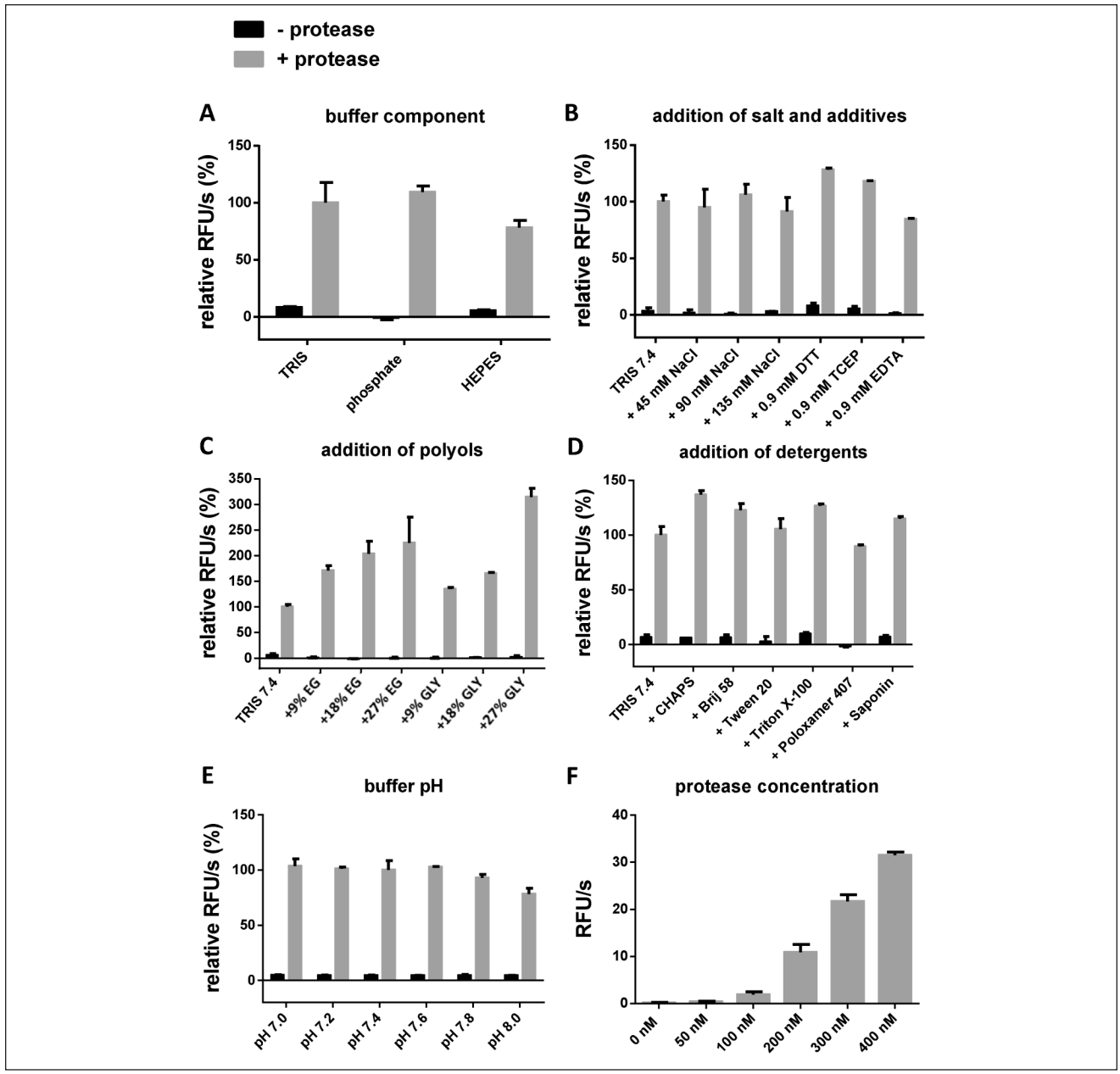

Figure 1. Buffer optimization of the FRET assay. The measurements were performed with substrate **4** (50 µM) and 500 nM enzyme concentration and at pH 7.4 unless indicated otherwise. Relative fluorescence units per second are given in comparison to the relative fluorescence units per second of the cleavage reaction in Tris buffer without additives. (**A**) Comparison of substrate cleavage velocity with different buffer components, pH 7.5. (**B**) Influence of salts and additives. (**C**) Influence of polyols. EG = ethylene glycol, Gly = glycerol. (**D**) Influence of detergents at a concentration of 0.009%. (**E**) Influence of pH (Tris buffer). (**F**) Different enzyme concentrations. All measurements were performed in triplicate.

cysteine residues may be scavenged by thiols in the assay buffer, thereby yielding false-negative results. Our results indicate that there is no necessity for thiols in the assay buffer, so that screening protocols may be implemented that allow the search for and characterization of thiol-reactive inhibitors with a covalent binding mode to the catalytic cysteine.

The chelating agent EDTA reduced the enzyme activity slightly. Using polyols as additives, we observed the highest enzymatic activities at high concentrations (**Fig. 1C**). Twenty-seven percent glycerol gave the highest enzymatic activity, probably by increasing the dimeric fraction of the protein, but it also causes high viscosity of the assay buffer and therefore has a detrimental effect on mixing and

A

Substrate	Sequence
1	2-Abz-Ser-Ala-Val-Leu-Gln||Ser-Gly-Tyr(3-NO_2)-Arg-OH
2	2-Abz-Ser-Val-Thr-Leu-Gln||Ser-Gly-Tyr(3-NO_2)-Arg-OH
3	2-Abz-Val-Val-Thr-Leu-Gln||Ser-Gly-Tyr(3-NO_2)-Arg-OH
4	2-Abz-Val-Val-Thr-Leu-Gln||Ser-Gly-Dap(Dnp)-Arg-OH
5	2-Abz-Ser-Val-Thr-Leu-His||Ser- Gly-Tyr(3-NO_2)-Arg-OH
6	2-Abz-Val-Leu-Gln||Ser- Gly-Tyr(3-NO_2)-OH
7	2-Abz-Nle-Lys-Arg-Arg-Ser-Tyr(3-NO_2)-NH_2
8	2-Abz-Gly-Lys-Lys-Arg-Gly-Tyr(3-NO_2)-Ala-Lys-NH_2

B

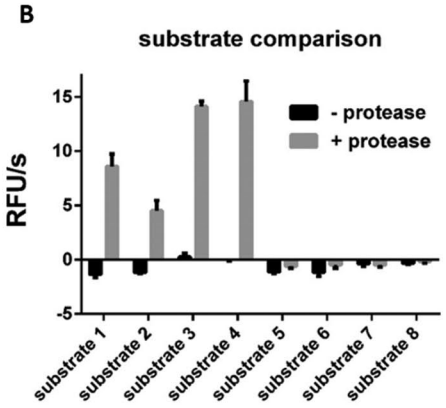

Figure 2. (**A**) The sequences of substrates **1–8**. (**B**) Comparison of cleavage rates of different substrates at 300 nM enzyme concentration. All measurements were performed in triplicate.

pipetting. A concentration of 18% ethylene glycol appears to combine high enzymatic activity with a negligible increase of viscosity. We also studied the effect of ionic and nonionic detergents on enzyme activity. All detergents were assayed at a concentration of 0.009%. Inclusion of detergents in the assay buffer can prevent the formation of colloidal aggregates that lead to nonspecific inhibition.[29–31] All detergents except poloxamer 407 increased the enzyme activity (**Fig. 1D**). The highest increase was measured with the zwitterionic detergent CHAPS. However, it should be considered that ionic functionalities may interact with charged functionalities of the test compounds, leading to false-negative results. Noting the absence of any larger dependence of enzymatic activity on detergent choice or presence, we decided to use Brij 58 at a concentration of 0.0016% for further experiments. This concentration is routinely used in viral and other protease assays in our laboratory in order to counteract promiscuous inhibition by aggregating compounds.

Furthermore, we tested the influence of different pH values on substrate cleavage velocity and found no significant influence in the pH range from 7.0 to 8.0 (**Fig. 1E**). A minimal decrease in activity can only be seen at a basic pH value higher than 7.6. Several publications described the influence of pH on enzyme activity of the SARS-CoV M^{pro}. Fan et al. and Tan et al. reported a peak of substrate cleavage at pH 7.0,[20,32] whereas other studies reported the highest processing at around pH 7.5[33] or pH 8.0.[28,34] Since the pH influences the conformation of the protease[20] and inhibitor recognition, a physiological pH value should be chosen. Additionally, various protease concentrations and the C145A mutant were investigated. The mutant protease was inactive (**Suppl. Fig. S1**). With increasing enzyme concentrations, the substrate cleavage increased significantly (**Fig. 1F, Suppl. Fig. S3**). A noticeable increase in enzymatic activity was observed between 100 and 200 nM, which is most likely due to formation of the catalytically competent homodimer that appears to start at around 100 nM (see **Suppl. Fig. S3** for a linear plot that demonstrates this concentration/activity dependency). For further studies, an enzyme concentration of 300 nM was chosen, which provides high signal intensity. We decided against higher enzyme concentrations in order to avoid hitting the "assay wall" in compound screening and characterization. DMSO in concentrations up to 6% had a negligible effect on enzymatic activity, as demonstrated in **Supplemental Figure S5**.

For further investigations, we used the combination of 300 nM enzyme, 50 mM Tris-HCl, pH 7.4, 100 mM NaCl, 20% ethylene glycol, and 0.0016% Brij 58 because this ensures a high activity of the protease as well as reliability and easy handling.

Substrate Characterization

After establishing the assay conditions, we proceeded with the investigation of the substrates. Eight FRET substrates were designed and synthesized, with *N*-terminal 2-aminobenzoic acid as a fluorophore (**Fig. 2A**). As a C-terminal quencher, either 3-nitrotyrosine (Tyr(3-NO_2)-OH; substrates **1**, **2**, **3**, **5**, and **6**) or *N*-beta-(2,4-dinitrophenyl)-L-2,3-diaminopropionic acid (L-Dap(Dnp)-OH; substrate **4**) was used. The substrates were synthesized by SPPS using the Fmoc strategy. The amino acid sequences were chosen based on the cleavage preferences of M^{pro} and substrates developed for SARS-CoV M^{pro} biochemical assays. Substrate **1** contains a truncated sequence from the FRET substrate DABCYL-KTSAVLQSGFRKME-EDANS, which was established for the assays of SARS-CoV M^{pro},[32,35] but also commonly used in the SARS-CoV-2 M^{pro} assays.[12,13,15,26,36] Substrate **2** was introduced by Blanchard et al. for the high-throughput

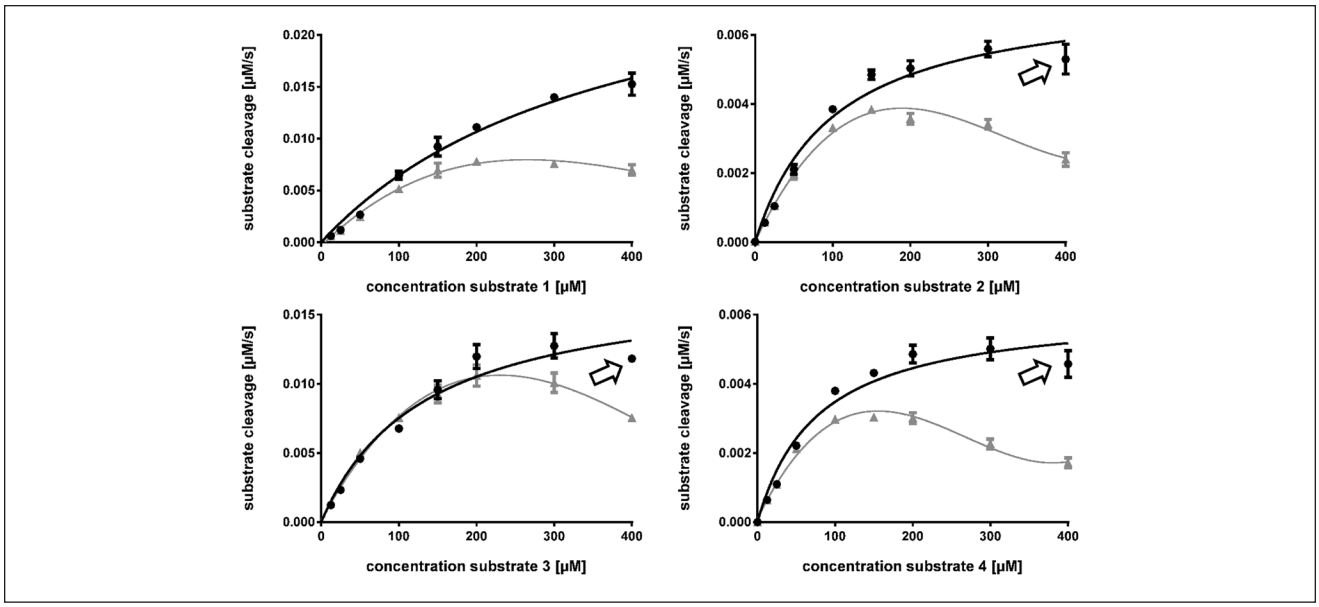

Figure 3. Michaelis–Menten curves for substrates **1–4** at SARS-CoV-2 M^{pro}. Gray curves with triangle markers were uncorrected for inner filter effects. Black curves with round markers were obtained upon inner filter effect correction.[41] Notice that at the highest tested concentration, substrates **2–4** show aberrant behavior, indicated by arrows, which is likely due to insufficient solubility or other effects (see discussion in the text). All measurements were performed in triplicate.

Table 1. K_m, V_{max}, K_{cat}, and K_{cat}/K_m Values for Different Substrates Determined by the FRET Assay, with Their Respective Errors (K_{cat}/K_m) and Standard Deviations (Other Quantities).

Substrate	1	2	3	4
K_m [μM]	536.3 ± 156.6	131.5 ± 25.9	197.9 ± 39.0	103.3 ± 18.5
V_{max} [μM/s]	0.0399 ± 0.0084	0.0084 ± 0.0007	0.0220 ± 0.0023	0.0071 ± 0.0005
K_{cat} [s^{-1}]	0.1330 ± 0.0279	0.0280 ± 0.0023	0.0733 ± 0.0077	0.0237 ± 0.0017
K_{cat}/K_m [M^{-1} s^{-1}]	248.0 ± 89.2	212.9 ± 45.5	370.4 ± 82.6	229.4 ± 44.2

All measurements were carried out in triplicate.

screening of inhibitors against SARS-CoV M^{pro},[37] while substrate **3** is a serendipitous discovery. In substrate **4**, the quencher 3-nitrotyrosine was replaced by Dap(Dnp)-OH in order to exclude potential fluctuations of fluorescence in the measurement, incurred from the use of an assay buffer with a similar pH value to the pKa value of the Tyr(3-NO_2)-OH side chain. Substrate **5** was previously recognized as a sequence not requiring glutamine at position P1,[38] whereas substrate **6** was designed to test the minimal sequence required for the recognition. Substrates **7** and **8** are substrates developed and routinely used in our group for the dengue virus and West Nile virus NS2B/NS3 protease assays, and they were used here as negative controls.[39,40]

We first screened the activity of the protease at a substrate concentration of 50 μM. The highest cleavage was observed for substrates **3** and **4** (**Fig. 2B**). These two substrates contain the amino acid sequence derived from the SARS-CoV M^{pro} substrate **2**, with a serendipitous replacement of serine for valine at position P5. This change caused an almost threefold increase in the cleavage of the substrate. Substrate **1** showed activity in between substrates **2** and **3** and **4**, whereas substrates **5**, with histidine at P1, and the minimal sequence substrate **6** had no activity. As expected, dengue virus and West Nile virus substrates (**7** and **8**) also exhibited no cleavage.

By determining K_m, V_{max}, K_{cat}, and K_{cat}/K_m values, we further characterized four substrates that displayed cleavage in the initial screening (**Fig. 3, Table 1**). In the calculations of K_m and V_{max}, we have included a correction for the inner filter effect of FRET pairs for each individual substrate (**Suppl. Tables S1–S4**).[39,41] An aberration of the curves was noticed for substrates **2–4** at the highest tested substrate concentration (400 μM; see arrows in **Fig. 3**), which appears to be unrelated to inner filter effects in the classical sense. We interpret this aberration as due to insufficient solubility at this (high) concentration, leading to the formation of

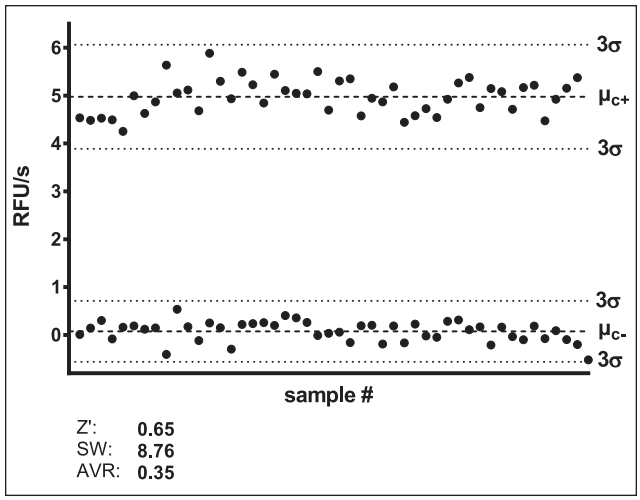

Figure 4. Z′ factor and signal window determination.

particles with unaccounted for absorption and diffraction behavior. The effect may also be caused by substrate inhibition. Consequently, the values at 400 μM were not used for the calculation of the kinetic parameters.

Substrate **3** showed the highest catalytic efficiency (K_{cat}/K_m), with a value 370.4 M^{-1} s^{-1}. Substrate **4**, with the same amino acid sequence but different quencher, had an almost twofold lower K_{cat}/K_m value of 229.4 M^{-1} s^{-1}. This was in the same range as for substrates **1** and **2**, with K_{cat}/K_m values of 248.0 M^{-1} s^{-1} and 212.9 M^{-1} s^{-1}, respectively. Substrate **4** showed the lowest K_m value, but also had the lowest V_{max}, whereas for substrate **1**, both values were the highest of the four characterized substrates. The K_{cat}/K_m value for substrate **1** is more than 10-fold lower than the values for the full-sequence equivalent substrate (DABCYL-KTSAVLQSGFRKME-EDANS) reported in the literature[13,26] (K_{cat}/K_m: SARS-CoV M^{pro}, 3011 M^{-1} s^{-1}; SARS-CoV-2 M^{pro}, 3426–6689 M^{-1} s^{-1}).

However, the full-sequence substrate showed comparable catalytic efficacy (214 M^{-1} s^{-1}) to our substrate **1** when measured with the native SARS-CoV-2 M^{pro} with the two extra residues histidine and methionine at the *N*-terminus.[26] Moreover, the truncated substrate TSAVLQSGFRK displayed similar catalytic efficacy (177 M^{-1} s^{-1}) at SARS-CoV M^{pro}.[32] The previously reported K_{cat}/K_m value for substrate **2** was 20 M^{-1} s^{-1} for SARS-CoV M^{pro}.[37] This is 10-fold lower than the value obtained in our assay; however, it has to be noted that in the previous work, the assay was performed in phosphate buffer without the addition of other components. This substrate has not been described on SARS-CoV-2 M^{pro} so far.

Z′ Score

The Z′-score determination for the assay was performed with substrate **1** at a protease concentration of 300 nM (**Fig. 4**). The calculated score of 0.65 indicates high reproducibility, robustness, and reliability of the assay. Furthermore, the score and a signal window greater than 2 demonstrate excellent assay performance and capability for high-throughput screenings.[21,22]

Reference Inhibitors

Substrate **1** was chosen for screening and IC_{50} determinations of the reference inhibitors (**Fig. 5, Table 2**). Three known inhibitors were selected as reference compounds according to their previously published activities against the proteases of SARS-CoV and SARS-CoV-2. The Food and Drug Administration (FDA)-approved hepatitis C protease inhibitor boceprevir was previously described as a potent covalent active-site inhibitor of SARS-CoV-2 M^{pro} with low micromolar IC_{50} values.[12,16,42] The thiophene chloropyridinyl ester MAC-5576 was identified as a potent SARS-CoV M^{pro} inhibitor in a high-throughput screening campaign.[37] Several structure–activity studies were carried out that led to improved inhibitory activity of the compound series.[43–45] The furoic ester FE-1 was detected as one of the most active SARS-CoV M^{pro} inhibitors. Furthermore, it was shown that both esters are active-site-directed covalent inhibitors.[43] In 2020, this compound

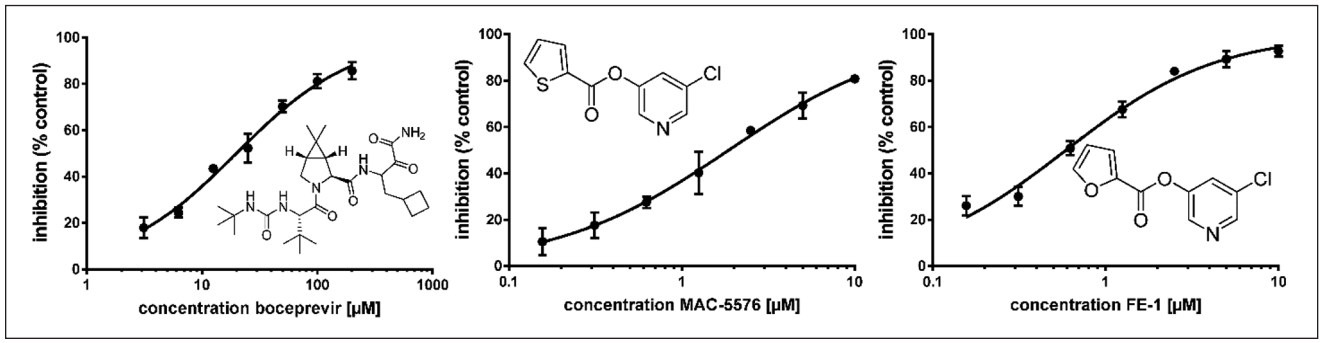

Figure 5. Dose–response curves and structures of reference compounds boceprevir (IC_{50} 19.9 ± 1.1 μM), MAC-5576 (IC_{50} 1.9 ± 0.05 μM), and FE-1 (IC_{50} 0.59 ± 0.04 μM). R^2 values for all curves are > 0.99. All measurements were performed in triplicate. Hill slopes: boceprevir, 0.85 ± 0.05; FE-1, 0.99 ± 0.07; MAC-5576, 0.87 ± 0.02.

Table 2. Inhibitory Activity of Reference Compounds against Isolated SARS-CoV-2 M^{pro} and Published IC_{50} Values against SARS-CoV and SARS-CoV-2 M^{pro}.

Compound	Screening: Inhibition @ 50 μM (%)[a]	IC_{50} SARS-CoV-2 M^{pro} (μM)[a]	K_i SARS-CoV-2 M^{pro} (μM)[b]	Published IC_{50} SARS-CoV M^{pro} (μM)	Published IC_{50} SARS-CoV-2 M^{pro} (μM)
Boceprevir	55.5 ± 4.7	19.9 ± 1.1	19.0	n.a.	4.1[12] 8.0[16] 5.4[42]
MAC-5576	96.1 ± 6.7	1.9 ± 0.05	1.8	0.5[37]	0.09[46]
FE-1	97.0 ± 4.1	0.59 ± 0.04	0.56	0.06[43]	n.a.

All measurements were carried out in triplicate. Screening at 50 μM and IC_{50} determinations were done separately. Dose–response curves of the IC_{50} determination are provided in **Figure 5**. n.a. = not available.
[a]Values against SARS-CoV-2 M^{pro} at 25 μM substrate and 300 nM enzyme concentration. [b]Calculated using the Cheng–Prusoff equation.

series was also described as active against the SARS-CoV-2 M^{pro} with a nanomolar IC_{50} value for compound MAC-5576.[46,47] Since all compounds are active-site inhibitors, IC_{50} value differences from the reference values are most likely due to different substrate concentrations and K_m values in the cited works. Additionally, IC_{50} values of covalent inhibitors are dependent on assay incubation times, which differed from assay to assay. K_i values for boceprevir, MAC-5576, and FE-1 were calculated using the Cheng–Prusoff equation. The observed K_i value of boceprevir (19 μM) differs from the literature value (1.18 μM),[12] which is very likely due to the different assay conditions.

To summarize, a systematic evaluation of assay conditions for the SARS-CoV-2 protease was performed in this work. It was shown that the assay performance with Tris and phosphate buffer is improved in comparison with HEPES buffer. The addition of salts had no influence on the protease activity, whereas polyols, as well as most of the tested detergents, improved activity. Six substrates were designed and tested under the newly established assay conditions. Substrate **1** with the FRET pair 2-Abz/Tyr(3-NO_2), which is a truncated version of the commonly used DABCYL-KTSAVLQSGFRKME-EDANS substrate, has been shown to be reliable and sufficiently active under the presented assay conditions and is suitable for performing high-throughput assays. By decreasing the size by five amino acid residues and replacing the DABCYL/EDANS FRET pair for the less expensive 2-Abz/Tyr(3-NO_2), it is possible to minimize the costs and time of the assay preparation, particularly in preparation of the substrate, while maintaining good performance. Furthermore, we have shown that in substrate **2**, a replacement of only one amino acid, that is, serine for valine at position P5, leads to an improved catalytic efficacy of the substrate. This observation also provides some additional insights to the general substrate—and possibly inhibitor—recognition properties of this enzyme and the main proteases of other coronaviruses with similar active sites.

Conclusion

We have developed a reliable and reproducible biochemical assay for the SARS-CoV-2 main protease, which can be applied in high-throughput screenings and focused characterization of inhibitors. We hope that the newly discovered conditions and substrates will aid in the development of potent antiviral compounds against SARS-CoV-2.

Acknowledgments

We thank Malte Hermes, Max Schmitt, Katharina Eckstein, and Aline Schöllkopf for their involvement in SARS-CoV-2 M^{pro} production. We also thank Tobias Haupt, Mathias Büchel, and Marie Hermann for preparing substrates **2**, **5**, and **6**, respectively; Heiko Rudy for measuring electrospray ionization mass spectrometry high-resolution spectra; and Natascha Stefan for technical assistance.

Declaration of Conflicting Interests

The authors declared no potential conflicts of interest with respect to the research, authorship, and/or publication of this article.

Funding

The authors received no financial support for the research, authorship, and/or publication of this article.

ORCID iDs

Christian D. Klein https://orcid.org/0000-0003-3522-9182
Nikos Kühl https://orcid.org/0000-0001-9025-7245

Supplemental Material

Supplemental material is available online with this article.

References

1. Hu, B.; Guo, H.; Zhou, P.; et al. Characteristics of SARS-CoV-2 and COVID-19. *Nat. Rev. Microbiol*. **2021**, *19*, 141–154.
2. Wu, F.; Zhao, S.; Yu, B.; et al. A New Coronavirus Associated with Human Respiratory Disease in China. *Nature* **2020**, *579*, 265–269.

3. Cui, J.; Li, F.; Shi, Z.-L. Origin and Evolution of Pathogenic Coronaviruses. *Nat. Rev. Microbiol*. **2019**, *17*, 181–192.
4. Huang, C.; Wang, Y.; Li, X.; et al. Clinical Features of Patients Infected with 2019 Novel Coronavirus in Wuhan, China. *Lancet* **2020**, *395*, 497–506.
5. Dong, E.; Du, H.; Gardner, L. An Interactive Web-Based Dashboard to Track COVID-19 in Real Time. *Lancet Infect. Dis*. **2020**, *20*, 533–534.
6. Wu, Z.; McGoogan, J. M. Characteristics of and Important Lessons from the Coronavirus Disease 2019 (COVID-19) Outbreak in China: Summary of a Report of 72 314 Cases from the Chinese Center for Disease Control and Prevention. *JAMA* **2020**, *323*, 1239–1242.
7. Cevik, M.; Kuppalli, K.; Kindrachuk, J.; et al. Virology, Transmission, and Pathogenesis of SARS-CoV-2. *BMJ* **2020**, *371*, m3862.
8. Ullrich, S.; Nitsche, C. The SARS-CoV-2 Main Protease as Drug Target. *Bioorg. Med. Chem. Lett*. **2020**, *30*, 127377–127377.
9. Grum-Tokars, V.; Ratia, K.; Begaye, A.; et al. Evaluating the 3C-Like Protease Activity of SARS-Coronavirus: Recommendations for Standardized Assays for Drug Discovery. *Virus Res*. **2008**, *133*, 63–73.
10. Jin, Z.; Du, X.; Xu, Y.; et al. Structure of Mpro from SARS-CoV-2 and Discovery of Its Inhibitors. *Nature* **2020**, *582*, 289–293.
11. Lee, J.; Worrall, L. J.; Vuckovic, M.; et al. Crystallographic Structure of Wild-Type SARS-CoV-2 Main Protease Acyl-Enzyme Intermediate with Physiological C-Terminal Autoprocessing Site. *Nat. Commun*. **2020**, *11*, 5877.
12. Ma, C.; Sacco, M. D.; Hurst, B.; et al. Boceprevir, GC-376, and Calpain Inhibitors II, XII Inhibit SARS-CoV-2 Viral Replication by Targeting the Viral Main Protease. *Cell Res*. **2020**, *30*, 678–692.
13. Zhang, L.; Lin, D.; Sun, X.; et al. Crystal Structure of SARS-CoV-2 Main Protease Provides a Basis for Design of Improved α-Ketoamide Inhibitors. *Science* **2020**, *368*, 409–412.
14. Dai, W.; Zhang, B.; Jiang, X.-M.; et al. Structure-Based Design of Antiviral Drug Candidates Targeting the SARS-CoV-2 Main Protease. *Science* **2020**, *368*, 1331–1335.
15. Hoffman, R. L.; Kania, R. S.; Brothers, M. A.; et al. Discovery of Ketone-Based Covalent Inhibitors of Coronavirus 3CL Proteases for the Potential Therapeutic Treatment of COVID-19. *J. Med. Chem*. **2020**, *63*, 12725–12747.
16. Fu, L.; Ye, F.; Feng, Y.; et al. Both Boceprevir and GC376 Efficaciously Inhibit SARS-CoV-2 by Targeting Its Main Protease. *Nat. Commun*. **2020**, *11*, 4417.
17. Vuong, W.; Khan, M. B.; Fischer, C.; et al. Feline Coronavirus Drug Inhibits the Main Protease of SARS-CoV-2 and Blocks Virus Replication. *Nat. Commun*. **2020**, *11*, 4282.
18. Ong, I. L. H.; Yang, K.-L. Recent Developments in Protease Activity Assays and Sensors. *Analyst* **2017**, *142*, 1867–1881.
19. Jares-Erijman, E. A.; Jovin, T. M. FRET Imaging. *Nat. Biotechnol*. **2003**, *21*, 1387–1395.
20. Tan, J.; Verschueren, K. H. G.; Anand, K.; et al. pH-Dependent Conformational Flexibility of the SARS-CoV Main Proteinase (M(pro)) Dimer: Molecular Dynamics Simulations and Multiple X-Ray Structure Analyses. *J. Mol. Biol*. **2005**, *354*, 25–40.
21. Iversen, P. W.; Eastwood, B. J.; Sittampalam, G. S.; et al. A Comparison of Assay Performance Measures in Screening Assays: Signal Window, Z′ Factor, and Assay Variability Ratio. *J. Biomol. Screen*. **2006**, *11*, 247–252.
22. Zhang, J.-H.; Chung, T. D. Y.; Oldenburg, K. R. A Simple Statistical Parameter for Use in Evaluation and Validation of High Throughput Screening Assays. *J. Biomol. Screen*. **1999**, *4*, 67–73.
23. Coelho, C.; Gallo, G.; Campos, C. B.; et al. Biochemical Screening for SARS-CoV-2 Main Protease Inhibitors. *PLoS One* **2020**, *15*, e0240079.
24. Gupta, Y.; Maciorowski, D.; Zak, S. E.; et al. Bisindolylmaleimide IX: A Novel Anti-SARS-CoV2 Agent Targeting Viral Main Protease 3CLpro Demonstrated by Virtual Screening Pipeline and In-Vitro Validation Assays. *Methods* **2021**. DOI: 10.1016/j.ymeth.2021.01.003.
25. Zhu, W.; Xu, M.; Chen, C. Z.; et al. Identification of SARS-CoV-2 3CL Protease Inhibitors by a Quantitative High-Throughput Screening. *ACS Pharmacol. Transl. Sci*. **2020**, *3*, 1008–1016.
26. Sacco, M. D.; Ma, C.; Lagarias, P.; et al. Structure and Inhibition of the SARS-CoV-2 Main Protease Reveal Strategy for Developing Dual Inhibitors against Mpro and Cathepsin L. *Sci. Adv*. 2020, *6*, eabe0751.
27. Hung, H.-C.; Ke, Y.-Y.; Huang, S. Y.; et al. Discovery of M Protease Inhibitors Encoded by SARS-CoV-2. *Antimicrob. Agents Chemother*. **2020**, *64*, e00872-20.
28. Graziano, V.; McGrath, W. J.; DeGruccio, A. M.; et al. Enzymatic Activity of the SARS Coronavirus Main Proteinase Dimer. *FEBS Lett*. **2006**, *580*, 2577–2583.
29. Feng, B. Y.; Shoichet, B. K. A Detergent-Based Assay for the Detection of Promiscuous Inhibitors. *Nat. Protoc*. **2006**, *1*, 550–553.
30. Feng, B. Y.; Shelat, A.; Doman, T. N.; et al. High-Throughput Assays for Promiscuous Inhibitors. *Nat. Chem. Biol*. **2005**, *1*, 146–148.
31. Seidler, J.; McGovern, S. L.; Doman, T. N.; et al. Identification and Prediction of Promiscuous Aggregating Inhibitors among Known Drugs. *J. Med. Chem*. **2003**, *46*, 4477–4486.
32. Fan, K.; Wei, P.; Feng, Q.; et al. Biosynthesis, Purification, and Substrate Specificity of Severe Acute Respiratory Syndrome Coronavirus 3C-Like Proteinase. *J. Biol. Chem*. **2004**, *279*, 1637–1642.
33. Huang, C.; Wei, P.; Fan, K.; et al. 3C-Like Proteinase from SARS Coronavirus Catalyzes Substrate Hydrolysis by a General Base Mechanism. *Biochemistry* **2004**, *43*, 4568–4574.
34. Chen, S.; Chen, L.-L.; Luo, H.-B.; et al. Enzymatic Activity Characterization of SARS Coronavirus 3C-Like Protease by Fluorescence Resonance Energy Transfer Technique. *Acta Pharmacol. Sin*. **2005**, *26*, 99–106.
35. Kuo, C.-J.; Chi, Y.-H.; Hsu, J. T. A.; et al. Characterization of SARS Main Protease and Inhibitor Assay Using a Fluorogenic Substrate. *Biochem. Biophys. Res. Commun*. **2004**, *318*, 862–867.

36. Zhang, L.; Lin, D.; Kusov, Y.; et al. α-Ketoamides as Broad-Spectrum Inhibitors of Coronavirus and Enterovirus Replication: Structure-Based Design, Synthesis, and Activity Assessment. *J. Med. Chem*. **2020**, *63*, 4562–4578.
37. Blanchard, J. E.; Elowe, N. H.; Huitema, C.; et al. High-Throughput Screening Identifies Inhibitors of the SARS Coronavirus Main Proteinase. *Chem. Biol*. **2004**, *11*, 1445–1453.
38. Goetz, D. H.; Choe, Y.; Hansell, E.; et al. Substrate Specificity Profiling and Identification of a New Class of Inhibitor for the Major Protease of the SARS Coronavirus. *Biochemistry* **2007**, *46*, 8744–8752.
39. Nitsche, C.; Klein, C. D. Fluorimetric and HPLC-Based Dengue Virus Protease Assays Using a FRET Substrate. In *Antiviral Methods and Protocols*, Gong, E. Y., Ed.; Humana Press: Totowa, NJ, **2013**; pp 221–236.
40. Kühl, N.; Graf, D.; Bock, J.; et al. A New Class of Dengue and West Nile Virus Protease Inhibitors with Submicromolar Activity in Reporter Gene DENV-2 Protease and Viral Replication Assays. *J. Med. Chem*. **2020**, *63*, 8179–8197.
41. Liu, Y.; Kati, W.; Chen, C.-M.; et al. Use of a Fluorescence Plate Reader for Measuring Kinetic Parameters with Inner Filter Effect Correction. *Anal. Biochem*. **1999**, *267*, 331–335.
42. Ghahremanpour, M. M.; Tirado-Rives, J.; Deshmukh, M.; et al. Identification of 14 Known Drugs as Inhibitors of the Main Protease of SARS-CoV-2. *ACS Med. Chem. Lett*. **2020**, *11*, 2526–2533.
43. Zhang, J.; Pettersson, H. I.; Huitema, C.; et al. Design, Synthesis, and Evaluation of Inhibitors for Severe Acute Respiratory Syndrome 3C-Like Protease Based on Phthalhydrazide Ketones or Heteroaromatic Esters. *J. Med. Chem*. **2007**, *50*, 1850–1864.
44. Niu, C.; Yin, J.; Zhang, J.; et al. Molecular Docking Identifies the Binding of 3-Chloropyridine Moieties Specifically to the S1 Pocket of SARS-CoV Mpro. *Biorg. Med. Chem*. **2008**, *16*, 293–302.
45. Ghosh, A. K.; Gong, G.; Grum-Tokars, V.; et al. Design, Synthesis and Antiviral Efficacy of a Series of Potent Chloropyridyl Ester-Derived SARS-CoV 3CLpro Inhibitors. *Bioorg. Med. Chem. Lett*. **2008**, *18*, 5684–5688.
46. Iketani, S.; Forouhar, F.; Liu, H.; et al. Lead Compounds for the Development of SARS-CoV-2 3CL Protease Inhibitors. *Nat. Commun*. **2021**, *12*, **2016**.
47. Hattori, S.-I.; Higshi-Kuwata, N.; Raghavaiah, J.; et al. GRL-0920, an Indole Chloropyridinyl Ester, Completely Blocks SARS-CoV-2 Infection. *mBio* **2020**, *11*, e01833-20.